Archival Report

Biological Psychiatry: CNNI

# Recovery-Associated Resting-State Activity and Connectivity Alterations in Anorexia Nervosa

Leon D. Lotter, Georg von Polier, Jan Offermann, Kimberly Buettgen, Lukas Stanetzky, Simon B. Eickhoff, Kerstin Konrad, Jochen Seitz, and Juergen Dukart

## ABSTRACT

**BACKGROUND:** Previous studies provided controversial insight on the impact of starvation, disease status, and underlying gray matter volume (GMV) changes on resting-state functional magnetic resonance imaging alterations in anorexia nervosa (AN). Here, we adapt a combined longitudinal and cross-sectional approach to disentangle the effects of these factors on resting-state alterations in AN.

**METHODS:** Overall, 87 female subjects were included in the study: adolescent patients with acute AN scanned at inpatient admission ($n$ = 22, mean age 15.3 years) and at discharge ($n$ = 21), patients who recovered from AN ($n$ = 21, mean age 22.3 years), and two groups of healthy age-matched control subjects (both $n$ = 22, mean age 16.0 and 22.5 years, respectively). Whole-brain measures of resting-state activity and functional connectivity were computed (network-based statistics, global correlation, integrated local correlation, and fractional amplitude of low-frequency fluctuations) to assess resting-state functional magnetic resonance imaging alterations over the course of AN treatment before and after controlling for underlying GMV.

**RESULTS:** Patients with acute AN displayed strong and widespread prefrontal, sensorimotor, parietal, temporal, precuneal, and insular reductions of resting-state connectivity and activity. All alterations were independent of GMV and were largely normalized in short-term recovered AN and absent in long-term recovered patients.

**CONCLUSIONS:** Resting-state functional magnetic resonance imaging alterations in AN constitute acute and GMV-independent, presumably starvation-related, phenomena. The majority of alterations found here normalized over the course of recovery without evidence for possible preexisting trait- or remaining "scar" effects.

https://doi.org/10.1016/j.bpsc.2021.03.006

Anorexia nervosa (AN) is a serious eating disorder (ED), typically occurring in females during puberty. It is characterized by a self-induced restriction of food intake and an intense fear of gaining weight, accompanied by a disturbed perception of one's own physical state (1). While the current literature agrees on an extensive biological foundation underlying the disorder, its nature has not yet been fully understood (2).

Resting-state functional magnetic resonance imaging (rsfMRI) (3) provides important insights into organization and alteration of functional brain networks. In contrast to task-based fMRI, rsfMRI is relatively simple to perform, easily scalable, and able to capture information on the brain network level independent of individual compliance and performance, thus promising to extend the current knowledge on neural alterations in AN (4). Previous rsfMRI research in AN led to a variety of findings, encompassing alterations of inter- as well as intraregional functional connectivity (FC) and activity in executive control, default mode, visual and sensorimotor networks as well as prefrontal and insular cortices (5–10). These alterations may underlie AN-related phenomena such as excessive cognitive control, disintegration of sensory and interoceptive information, and persistent rumination about topics related to body weight and body shape (5).

The often severe starvation that patients experience in the acute state of AN can cause various somatic and psychiatric symptoms that are not necessarily a specific product of the disorder but of starvation in general (2). The physical adaptation to starvation may be partly regulated by leptin, a hormonal marker of adiposity and energy storage (11). As was shown for gray matter volume (GMV) during different weight-recovery states of AN (12,13), causes and consequences of undernutrition can influence resting-state brain functioning (14,15). Longitudinal studies are crucial to better understand the development of rsfMRI alterations during the clinical course of AN and to disentangle the contribution of starvation and weight restoration from potential specific AN traits. Only two studies to date adapted such a longitudinal design providing controversial results on FC alterations (16,17). While Cha *et al.* (16) reported FC differences to disappear after short-term weight restoration, Uniacke *et al.* (17) found some evidence for persistent FC alterations. In line with the latter, alterations in executive control (18), default mode (19), and visual networks (20,21) were reported in long-term recovered patients. However, these findings were not consistently replicated (5,6), may have been confounded by differences in underlying gray matter (22), and were questioned by a recent larger-scale study

 

ISSN: 2451-9022

(23) reporting a normalization of most alterations found in acute AN (7).

To date, owing to widespread and inconsistent findings obtained by a variety of data analytic methods with mostly cross-sectional approaches, the questions on the nature (e.g., relation between intra- and interregional FC alterations), confounds (e.g., influence of GMV changes), and state- or trait dependency (influence of acute malnutrition) of rsfMRI alterations in AN remain open.

To address these questions, we examined rsfMRI data in patients in the underweight, short-term weight-restored, and long-term recovered state of AN. Given the widespread nature of previous findings, we followed a data-driven approach testing for alterations of whole-brain FC and activity by utilizing network-based statistics (NBS) (24), global correlation (GC) (25), integrated local correlation (LC) (26), and the fractional amplitude of low-frequency fluctuations (fALFF) (27). We further evaluated whether rsfMRI alterations persist when controlling for underlying GMV. Using this integrative approach, we aimed to provide valuable insights into the development of resting-state alterations over the clinical course of AN.

## METHODS AND MATERIALS

### Participants

In total, 87 women underwent rsfMRI scanning in two separate cohorts (Table 1; Tables S1–S3). The first cohort (acu) comprised 22 adolescent inpatients with AN ($n$ = 1 binge eating/purging subtype) who were scanned at admission (T1acu) and after discharge from treatment (T2acu, $n$ = 21) along with 22 age-matched healthy control (HC) subjects (HCacu; scanned once). The second cohort (rec) consisted of 21 young adult patients recovered from adolescent-onset AN for at least 12 months (T3rec) and 22 age-matched HC subjects (HCrec). Except for 3 patients with AN, the two cohorts comprised separate participants. To avoid any additional assumptions on the data, the cohorts were assumed independent. AN was diagnosed according to DSM-5 criteria (1), and all patients received inpatient treatment at the ED unit of the Department of Child and Adolescent Psychiatry and Psychotherapy, University Hospital Aachen, Aachen, Germany. For additional details on the study sample as well as recruitment and scanning procedure, see Supplemental Methods.

Both studies were approved by the local ethics committee (cohort 1: EK081/10, cohort 2: EK213/15) and were conducted in accordance with the Declaration of Helsinki. All participants and their legal guardians (if underage) gave written informed consent.

### Clinical Assessments

Current ED diagnosis and severity were examined using the Eating Disorder Examination (28) and the Eating Disorder Inventory-2 (EDI-2; 6-point scale, 11 subscales) (29). Undernutrition was quantified by age- and sex-adjusted body mass index–standard deviation score (BMI-SDS) (30,31) and plasma leptin. The sex adjustment of BMI scores was relevant to evaluating the participant's nominal underweight (see Supplemental Methods). Symptoms of depression were assessed with the Beck Depression Inventory (BDI) (32). Screening for psychiatric comorbidities was conducted using the Kiddie Schedule for Affective Disorders and Schizophrenia (33) or the Mini-International Neuropsychiatric Interview (34). The Multiple-choice Vocabulary Test (35) was utilized to approximate verbal intelligence quotient. Further information on psychopathology and past inpatient treatments was obtained from clinical records. Interviews were conducted by specifically trained and supervised clinical researchers with background in medicine or psychology.

### MRI Data Acquisition

All participants were scanned at the same 3T MRI scanner (Magnetom Prisma; Siemens, Erlangen, Germany). Structural T1-weighted images were acquired using a magnetization prepared rapid acquisition gradient-echo (MPRAGE) sequence with following parameters: cohort 1: repetition time = 1880 ms, echo time = 3.03 ms, and field of view = 256 × 256 mm; cohort 2: repetition time = 2300 ms, echo time = 2.98 ms, and field of view = 256 × 240 mm; both cohorts: number of slices = 176 and voxel size = 1 × 1 × 1 $mm^3$. For rsfMRI, all probands underwent a 7-minute eyes-closed T2*-weighted gradient-echo echo planar imaging protocol with repetition time = 2000 ms, echo time = 28 ms, flip angle = 77°, field of view = 192 × 192 mm, number of slices = 34, number of volumes = 210, and voxel size = 3 × 3 × 3.5 $mm^3$. All subjects in cohort 1 (patients and HC subjects) were scanned during daytime while continuing their usual food intake or refeeding plans; all subjects in cohort 2 were scanned in the morning after an overnight fasting.

### Preprocessing

Preprocessing of functional and structural images was conducted with SPM12 (36) in a MATLAB, version R2018a (The MathWorks, Inc., Natick, MA) environment. For further processing and analyses of rsfMRI data, CONN18b (25) was used.

Preprocessing included removal of the first four frames, realignment for motion correction and coregistration to structural images with subsequent spatial normalization into Montreal Neurological Institute space using parameters derived from structural data, and interpolation of the data to a 3-mm isotropic resolution. The normalization parameters were also applied (with modulation) to segmented gray matter probability maps to obtain corresponding voxelwise GMV. A gray matter mask (probability of gray matter > 0.2) was applied to all images to restrict analyses to gray matter tissue. A Gaussian smoothing kernel of 6-mm full width at half maximum was applied to rsfMRI data. Twenty-four motion parameters (37) along with mean white matter and cerebrospinal fluid signals were regressed out of the functional data. The resulting images were linearly detrended and temporally bandpass filtered (0.01–0.08 Hz). One HCacu had to be excluded from analyses because of data processing errors. Groups did not differ in regard to mean framewise displacement (FWD) and no subject exceeded a maximum FWD (translation) of 3 mm (Table S4).

### Analyses of Demographic and Clinical Data

Statistical analyses of demographic and clinical data were conducted using R, version 3.6.1. (38) and *jamovi,* version 1.2

**Table 1. Demographic and Clinical Sample Characteristics**

| Characteristics | T1acu, Admission, *n* = 22 | T2acu, Discharge, *n* = 21 | HCacu, *n* = 22 | T3rec, Recovery, *n* = 21 | HCrec, *n* = 22 |
|---|---|---|---|---|---|
| General | | | | | |
| Age, years | 15.3 ± 1.9 (10.2 to 18.6) | 15.5 ± 2.0 (10.5 to 18.9) | 16.0 ± 2.0 (12.8 to 19.2) | 22.3 ± 3.3 (17.7 to 31.4) | 22.5 ± 3.5 (16.6 to 31.3) |
| Verbal IQ | 108.9 ± 17.0 (92 to 143)[a] | – | 98.0 ± 9.7 (82 to 124) | 108.2 ± 9.5 (97 to 124) | 110.9 ± 12.0 (95 to 130) |
| ED Severity | | | | | |
| BMI, kg/m$^2$ | 15.7 ± 1.5 (13.1 to 18.3)[a,b] | 18.2 ± 1.2 (15.0 to 20.1)[a] | 22.3 ± 2.1 (18.7 to 26) | 21.8 ± 2.6 (18.6 to 26.6) | 21.9 ± 2.0 (19.1 to 25.5) |
| BMI-SDS | –2.7 ± 1.4 (–5.5 to –1.0)[a,b] | –1.1 ± 0.4 (–1.9 to –0.5)[a] | 0.3 ± 0.6 (–1.1 to 1.1) | –0.3 ± 0.8 (–1.4 to 0.9) | –0.2 ± 0.7 (–1.2 to 0.9) |
| Leptin, ng/mL | 2.0 ± 1.8 (0.9 to 6.9)[a,b] | 6.0 ± 3.9 (0.9 to 14)[a] | 20.0 ± 12.0 (6.6 to 48) | 12.6 ± 7.2 (3.7 to 26) | 11.1 ± 6.4 (2.8 to 25.6) |
| ED History | | | | | |
| Age at ED onset, years | 13.9 ± 1.9 (9.1 to 17.9) | – | – | 14.4 ± 1.6 (11.8 to 17.6) | – |
| Age at (first) admission, years | 15.2 ± 2 (10.2 to 18.6) | – | – | 15.2 ± 1.6 (12.0 to 18.4) | – |
| BMI at admission/discharge, kg/m$^2$ | 15.3 ± 1.3 (12.6 to 18.4) | 18.4 ± 1.2 (15.5 to 20.2) | – | 15.7 ± 2.1 (11.3 to 21.3) | – |
| BMI-SDS at admission/discharge | –2.9 ± 1.2 (–5 to –1.4) | –1.0 ± 0.4 (–1.8 to –0.5) | – | –2.7 ± 1.5 (–6.2 to –0.2) | – |
| Time from T1 to T2, days | – | 90.8 ± 40.8 (41 to 183) | – | – | – |
| ED duration, years[c] | 1.6 ± 1.3 (0.5 to 4.8) | – | – | 2.0 ± 1.7 (0.1 to 7.1) | – |
| Recovery duration, years[d] | | – | – | 5.3 ± 3.0 (1.5 to 13.2) | – |
| Time from admission to T1/time from T2 to discharge, days | 19.6 ± 12.3 (4 to 60) | 8.1 ± 26.1 (–52 to 52) | – | – | – |
| Symptom Scales | | | | | |
| EDE mean total score | 3.8 ± 1.2 (1.6 to 5.7)[b] | 2.0 ± 1.1 (0.3 to 4.4) | – | 1.0 ± 1.0 (0.1 to 3.7) | – |
| EDI-2 total score | 271.5 ± 80.1 (109 to 436)[a] | 252.5 ± 58.9 (106 to 335)[a] | 187.4 ± 31.9 (115 to 240) | 259.8 ± 73.2 (175 to 399)[a] | 194.6 ± 32.8 (151 to 263) |
| BDI-2 total score | 18.4 ± 13.6 (0 to 38)[a] | 13.5 ± 14.2 (0 to 51)[a] | 3.1 ± 2.7 (0 to 10) | 10.7 ± 11.5 (0 to 37)[a] | 3.9 ± 3.9 (0 to 12) |

Values are presented as mean ± SD (range). $\alpha = .05$, $p$ uncorrected. For detailed results of statistical comparisons, see Table S1; for additional sample information, see Table S3.

Missing data: T1acu: verbal IQ: $n = 6$, EDE: $n = 3$, EDI-2: $n = 1$, BDI-2: $n = 3$. T2acu: leptin: $n = 1$, EDE: $n = 3$, EDI-2: $n = 4$, BDI-2: $n = 3$. T3rec: age at ED onset: $n = 12$, BMI-SDS at first admission: $n = 1$. HCrec: verbal IQ: $n = 1$, EDI-2: $n = 2$, BDI-2: $n = 1$.

acu, acute; BDI-2, Beck Depression Inventory-II; BMI-SDS, body mass index-standard deviation score; ED, eating disorder; EDE, Eating Disorder Examination; EDI-2, Eating Disorder Inventory-2; HC, healthy control; rec, recovered.

[a]Significant difference compared with HC subjects (T1acu/T2acu vs. HCacu or T3rec vs. HCrec).

[b]Significant difference compared with T2acu. $\alpha = .05$, $p$ uncorrected.

[c]ED duration was calculated as time from symptom onset to last discharge (if symptom onset not available, from first admission).

[d]Recovery duration was calculated as time from last inpatient discharge or last underweight state to examination.

(39). To compare characteristics between groups, *t* test, Mann-Whitney-*U* test, or Wilcoxon test were used, as appropriate.

## Primary Analyses of rsfMRI Data

Primary rsfMRI analyses consisted of 1) calculation of resting-state FC and activity measures based on whole-brain voxelwise data and 2) a parcellation-based approach applying NBS (24). The derived measures were compared between AN and corresponding HC groups (T1acu vs. HCacu, T2acu vs. HCacu, T3rec vs. HCrec) and between T1acu and T2acu to assess temporal evolution of rsfMRI alterations in the acute-to-recovery phase. In addition, an interaction design including acute and recovered patients and corresponding control groups was applied, testing for group-by-time interactions between patients at admission and in long-term recovery. Extraction of voxelwise rsfMRI measures and calculation and visualization of NBS results were conducted using CONN.

GC was calculated as the average of bivariate correlations between the blood oxygenation level–dependent signal of a given voxel and every other voxel (25). LC was computed as the average bivariate correlation between each voxel and its neighboring voxels weighted by a Gaussian convolution with 6-mm full width at half maximum (26). fALFF was calculated at each voxel as the root mean square of the blood oxygenation level–dependent signal amplitude in the analysis frequency band (0.01–0.08 Hz) divided by the amplitude in the entire frequency band (27). Group comparisons were conducted using *t* contrasts within general linear models while controlling for age. Data from T1acu were compared with those from T2acu using a repeated-measures design. An exact permutation-based (1000 permutations) cluster threshold ($p < .05$) was applied in all analyses combined with an uncorrected voxelwise threshold of $p < .01$ (22), allowing for an accurate control of the false-positive rate while maintaining sensitivity to potentially weak resting-state alterations (40).

For NBS analyses, preprocessed functional images were (without smoothing) parcellated into 100 cortical (41) and 16 subcortical brain regions (Neuromorphometrics, Inc.). For reporting, Automated Anatomical Labeling atlas (42) regions corresponding to the centroid coordinates of the Schaefer-atlas were used. Blood oxygenation level–dependent signal time courses were averaged within each region of interest (ROI). Subjectwise bivariate correlation matrices ($116 \times 116$) were calculated and Fisher's *z*–transformed. Each ROI-to-ROI connection was compared between groups, and resulting *p* values were thresholded at an uncorrected level of $p < .01$. Within this set of suprathreshold connections, all possible connected (sub-)networks were identified. Using permutation testing (10,000 iterations), resulting subnetworks were assessed for statistical significance based on their sizes while controlling the familywise error rate (24).

In additional sensitivity analyses, contrasts yielding significant group differences were recomputed by including mean rotational and translational FWD as additional covariates to control for motion at the group level.

## Post Hoc Group Comparisons

Implementation and visualization of post hoc comparisons and correlation analyses were conducted using *jamovi* and R. To better understand group differences, FC of every connection included in significant NBS subnetworks was averaged for each subnetwork (separately for increased and decreased connections), and values of every voxel included in significant clusters were averaged per cluster. These measures representing whole networks or clusters, respectively, were used for further analyses. Age was controlled for in all post hoc analyses. The correction for multiple comparisons inherent to the NBS procedure does not allow for inference about individual connections (24). To explore the neuroanatomy of the NBS results, the region with the strongest alteration in node degree (the region showing the largest number of altered connections) in each subnetwork was identified. Connections between these regions and any other ROI that showed significant differences (Bonferroni-corrected) between groups were identified by applying a seed-to-ROI approach.

To illustrate the temporal development of resting-state properties that were altered in acute AN, averaged values from the T1acu < HCacu and T1acu < T2acu contrasts were compared between AN and corresponding HC using analyses of covariance or paired *t* tests for each network or cluster. To demonstrate that altered functional connections and clusters coinciding between different contrasts showed consistent recovery dynamics, overlapping FC and voxelwise values were extracted and compared as stated above. Bonferroni correction was applied to control for the number of tests per rsfMRI modality and contrast. To test for statistical biases and to allow for an appropriate interpretation of the results when comparing data based on the T1acu versus HCacu comparison between T2acu and the same control group, we performed a simulation experiment. Results indicated that the likelihood of observing significant between-group differences increases for such comparisons (see Supplemental Methods, Supplemental Results, and Figure S3). In additional sensitivity analyses, we explored the effects of controlling for IQ, for time between inpatient admission and T1 (to control for delayed scanning), and for BMI-SDS, as well as effects of excluding participants taking psychoactive medication. To evaluate the potential impact of outliers on rsfMRI group differences, we recalculated corresponding post hoc group comparisons using nonparametric statistics (see Supplemental Methods and Supplemental Results).

## Relationships Among rsfMRI Measures

We further assessed how the different rsfMRI alterations identified in acute AN relate to each other. For this, Pearson correlations between all rsfMRI measures in AN at T1 as well as between changes in rsfMRI measures from T1 to T2 were computed (false discovery rate–corrected).

## Relationship to Clinical Outcomes

Next, we tested for associations between rsfMRI results and clinical variables. Pearson correlations (Bonferroni-corrected) were computed between rsfMRI alterations (T1acu vs. HCacu and delta T2-T1) and BMI-SDS, leptin, total scores on Eating Disorder Examination, EDI-2 and BDI-2, the time between ED onset and inpatient admission (T1acu), and the time from T1 to T2 (delta T2-T1).

### Effects of GMV on rsfMRI Alterations

To evaluate the impact of GMV on rsfMRI alterations, voxelwise GMV was averaged for each cluster or subnetwork from resting-state analyses and compared between groups using analyses of covariance or paired *t* tests where appropriate. To evaluate influences of GMV changes on NBS results, group comparisons were recomputed after GMV was regressed out of the averaged network FC (separately for acute and recovered cohorts). For voxelwise rsfMRI measures, individual GMV was regressed out at each voxel included in significant clusters. Cluster values were then averaged and compared between groups. To assess the impact of GMV correction on the magnitude of resting-state group differences, Cohen's *d* values (with Hedge's *g* correction) were computed for all significant rsfMRI measures before and after controlling for GMV (along with respective GMV effect sizes).

## RESULTS

### Demographic and Clinical Sample Characteristics

AN patients and corresponding HC subjects did not differ regarding age. In cohort 1, patients with AN showed higher verbal IQ than HC subjects. Patients from the two study cohorts were comparable with regard to age at ED onset as well as age and BMI-SDS at first inpatient admission. As expected, patients with AN at T1 showed significantly lower BMI (-SDS) and leptin levels and higher scores on Eating Disorder Examination, EDI-2, and BDI-2. Average BMI increase during inpatient treatment was 20.8% ± 9.5%. T3rec patients exhibited elevated EDI-2 scores (Table 1; Tables S1 and S2).

### Parcellation-Based Results

Using NBS, we identified significant differences between T1acu and HCacu and between T1acu and T2acu (Figure 1A, C; see 3D neuroimaging content online for Figures S1 and S2; see also Table S5). Included connections were largely decreased for T1acu constituting a widespread network across the whole brain. T2acu as well as T3rec patients did not differ from HC subjects. Post hoc analyses based on T1acu findings revealed smaller but significant FC reduction for T2acu but not for T3rec (Figure 1E–G; Table S6).

Left anterior superior frontal gyrus (T1acu vs. HCacu subnetwork) (see 3D neuroimaging content online for Figure S2A) and left insular cortex (T1acu vs. T2acu subnetwork) (see 3D

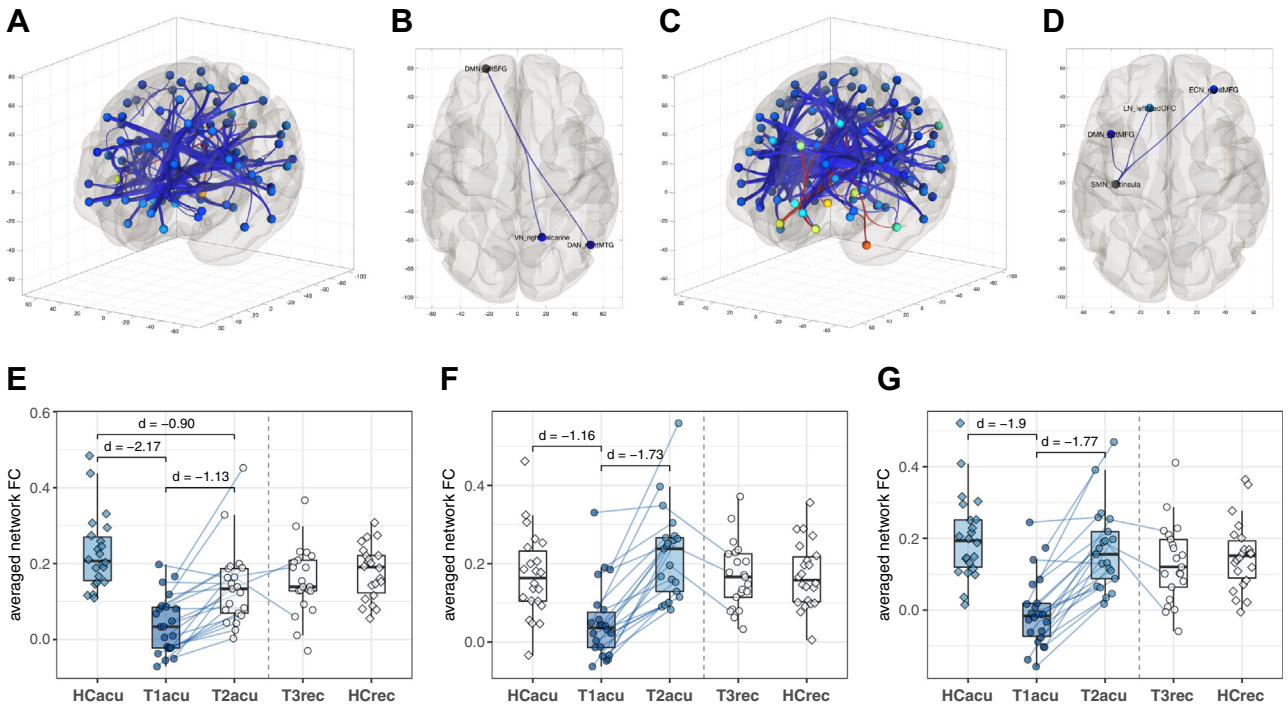


**Figure 1.** Network-based statistics. **(A)** Network-based statistics subnetwork resulting from T1acu vs. HCacu comparison. **(B)** Seed-to-region of interest: within the T1acu vs. HCacu subnetwork, functional connectivity (FC) between the left superior frontal gyrus (seed) and right calcarine sulcus/middle temporal gyrus shows the strongest reduction ($p < .05/115$). **(C)** Network-based statistics subnetwork resulting from T1acu vs. T2acu comparison. **(D)** Seed-to-region of interest: within the T1acu vs. T2acu subnetwork, FC between the left insula (seed) and prefrontal regions (middle frontal and orbitofrontal gyri) shows the strongest reduction. **(E)** Post hoc comparison of averaged T1acu < HCacu subnetwork FC. **(F)** Post hoc comparison of averaged T1acu < T2acu subnetwork FC. **(G)** Post hoc comparison of subnetwork FC averaged from connections overlapping between T1acu < HCacu and T1acu < T2acu subnetworks. Boxplot figures represent post hoc comparisons of results from T1acu < HCacu and T1acu < T2acu contrasts. Each box represents one group; the scatter points represent single subjects (anorexia nervosa subjects as circles, healthy control subjects as squares). Blue lines indicate matching values of individual anorexia nervosa subjects. The groups involved in the original, primary comparisons are colored to highlight circular statistical tests. Only groups within each study cohort were compared with each other; the dashed line separates the cohorts. Significant group comparisons (Bonferroni-corrected) are marked with brackets and complemented by corresponding effect sizes (Cohen's *d*, Hedge's *g* corrected). acu, acute; DMN, default mode network; ECN, executive control network; HC, healthy control; medOFC, medial orbitofrontal cortex; MFG, middle frontal gyrus; rec, recovered; SMN, sensorimotor network; T, time.

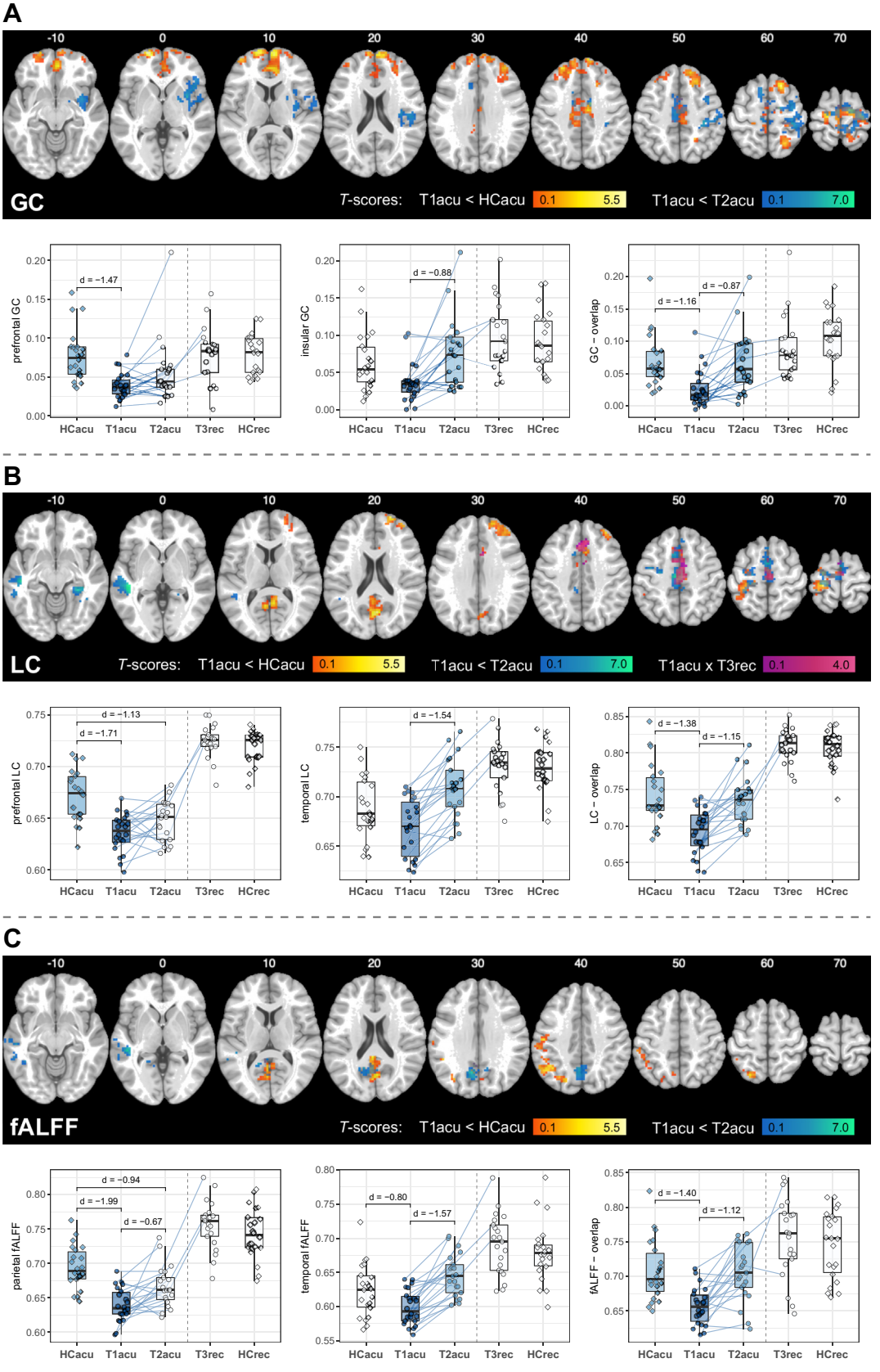
A
GC
T-scores: T1acu < HCacu 0.1 5.5 T1acu < T2acu 0.1 7.0
prefrontal GC
insular GC
GC – overlap
B
LC
T-scores: T1acu < HCacu 0.1 5.5 T1acu < T2acu 0.1 7.0 T1acu x T3rec 0.1 4.0
prefrontal LC
temporal LC
LC – overlap
C
fALFF
T-scores: T1acu < HCacu 0.1 5.5 T1acu < T2acu 0.1 7.0
parietal fALFF
temporal fALFF
fALFF – overlap
HCacu T1acu T2acu T3rec HCrec

neuroimaging content online for Figure S2B) displayed the largest decreases in node degree. Using these seeds, we found decreased FC in T1acu between left superior frontal gyrus and ROIs in the left medial temporal gyrus and right calcarine sulcus as well as between the left insula and bilateral medial frontal and left medial orbitofrontal cortices (Figure 1B, D; Table S5). NBS results were largely similar when additionally controlling for FWD, IQ, admission scan delay, and BMI-SDS, when excluding participants taking psychoactive medication or when using nonparametric statistics (Tables S7–S12).

## Voxelwise Results

In pairwise comparisons, significant differences were observed for all voxelwise resting-state measures for T1acu < HCacu and T1acu < T2acu contrasts (Figure 2A–C, brain slices; Table S13). No other contrasts were significant. T1acu patients exhibited reduced GC in bilateral prefrontal regions in comparison with HC subjects and in the right insula relative to T2acu (Figure 2A). In both contrasts, GC was reduced in bilateral sensorimotor areas. LC was reduced in T1acu in bilateral sensorimotor areas, right SFG, and bilateral precuneus relative to HCacu and in bilateral sensorimotor, right fusiform, and left medial temporal gyrus areas relative to T2acu (Figure 2B). We found a significant interaction in the medial posterior frontal cortex for LC comparing T1acu and T3rec patients relative to respective HC subjects (Figure 2B). fALFF was reduced for T1acu in bilateral precuneus and calcarine sulcus compared with T2acu and HCacu, in left parietal regions relative to HCacu, and in left medial temporal gyrus relative to T2acu (Figure 2C).

From all identified clusters per modality, (right) prefrontal GC and LC and left parietal fALFF showed the largest effect sizes (Figure 2A–C, left boxplot diagrams and 3C; Table S6). In post hoc group comparisons of these clusters, the right prefrontal LC and left parietal fALFF were also reduced in T2acu compared with HCacu (Figure 2B, C, left boxplot diagrams; Table S6). Brain areas coinciding between the significant contrasts showed reductions for T1acu compared with both HCacu and T2acu for all modalities (Figure 2A–C, right boxplot diagrams; Table S6). All results remained largely similar when controlling for FWD, IQ, and admission scan delay or when excluding medicated participants (Tables S8, S9, S11, and S14). When controlling for BMI-SDS in the T1acu < HCacu contrast, only alterations in prefrontal GC and LC and left parietal fALFF remained significant; in the T1acu < T2acu contrast, all differences, except sensorimotor GC, remained significant (Table S10). Outliers in the data did not have significant impact on group effects (Table S12).

## Correlations Among rsfMRI Measures

Considering the multitude of identified alterations, we explored which of the observed rsfMRI changes were related to each other using correlation analyses. We found strong positive correlations between measures capturing global (NBS, GC) and local (LC, fALFF) resting-state characteristics and between topologically close alterations obtained by different methods (e.g., GC and LC in prefrontal or motor areas). Changes in rsfMRI measures from T1 to T2 correlated strongly across all measures, except for T1acu > HCacu and T1acu > T2acu network FC and prefrontal LC (Figure 3A).

## Relationship to Clinical Outcomes

No correlations between rsfMRI results and clinical variables remained significant after correction for multiple comparisons (Table S15). At an uncorrected $p < .05$, in patients with acute AN, T1acu < HCacu network FC was positively associated with EDI-2 scores. Bilateral precuneal LC was positively correlated with BMI-SDS, EDI-2, and BDI-2 in patients with acute AN. Changes in right fusiform LC and left temporal fALFF correlated positively with time from T1 to T2 (Figure 3B). Given the unexpected direction of correlations with global ED severity scores, we performed additional exploratory correlation analyses that suggested strongest correlations between FC changes and EDI-2 subscales such as maturity fear and social insecurity rather than core eating behavior abnormality subscales (Supplemental Results and Figure S4).

## Effects of GMV on rsfMRI Alterations

GMV was significantly reduced in acute AN in all rsfMRI clusters and networks (Figure 3C; Table S16). When regressing GMV out of voxelwise GC, LC, and fALFF maps or averaged network FC, group differences and corresponding effects sizes remained largely unchanged for all measures (Figure 3C; Table S17). GMV did not correlate with any of the rsfMRI measures (Table S18).

# DISCUSSION

We systematically explored whole-brain rsfMRI alterations in acute, short-term and long-term recovered, adolescent-onset AN. In patients with acute AN, we found spatially widespread decreases of local and global FC and local activity measures. These alterations were independent of underlying GMV and normalized largely with short-term weight restoration to being absent in the long-term recovered group.

In line with several previous publications, we found largely decreased intra- and interregional rsfMRI measures in acute

**Figure 2.** Voxelwise functional connectivity and activity. Brain slices: clusters of significantly reduced voxelwise resting-state measures in T1acu patients compared with HCacu (red-yellow) and compared with T2acu (blue-green); results from T1acu < HCacu × T3rec > HCrec contrast are displayed in purple. Color brightness reflects T-value size at a given voxel. Boxplot diagrams: left and middle: clusters with the largest effect sizes in post hoc comparisons of each voxelwise resting-state measure. Right: post hoc comparisons of clusters overlapping between T1acu < HCacu and T1acu < T2acu contrasts. For general descriptions of the boxplot diagrams, refer to the legend of Figure 1. **(A)** Global correlation (GC). Alterations of prefrontal (T1acu < HCacu) and right insula GC (T1acu < T2acu) show the largest effect sizes. **(B)** Integrated local correlation (LC). The largest effect sizes were observed for LC in the right superior frontal gyrus (T1acu < HCacu) and in the left middle temporal gyrus (T1acu < T2acu). **(C)** Fractional amplitude of low-frequency fluctuations (fALFF). Left parietal fALFF (T1acu < HCacu) and fALFF in left middle temporal gyrus (T1acu < T2acu) display the largest effect sizes. acu, acute; HC, healthy control; rec, recovered; T, time.

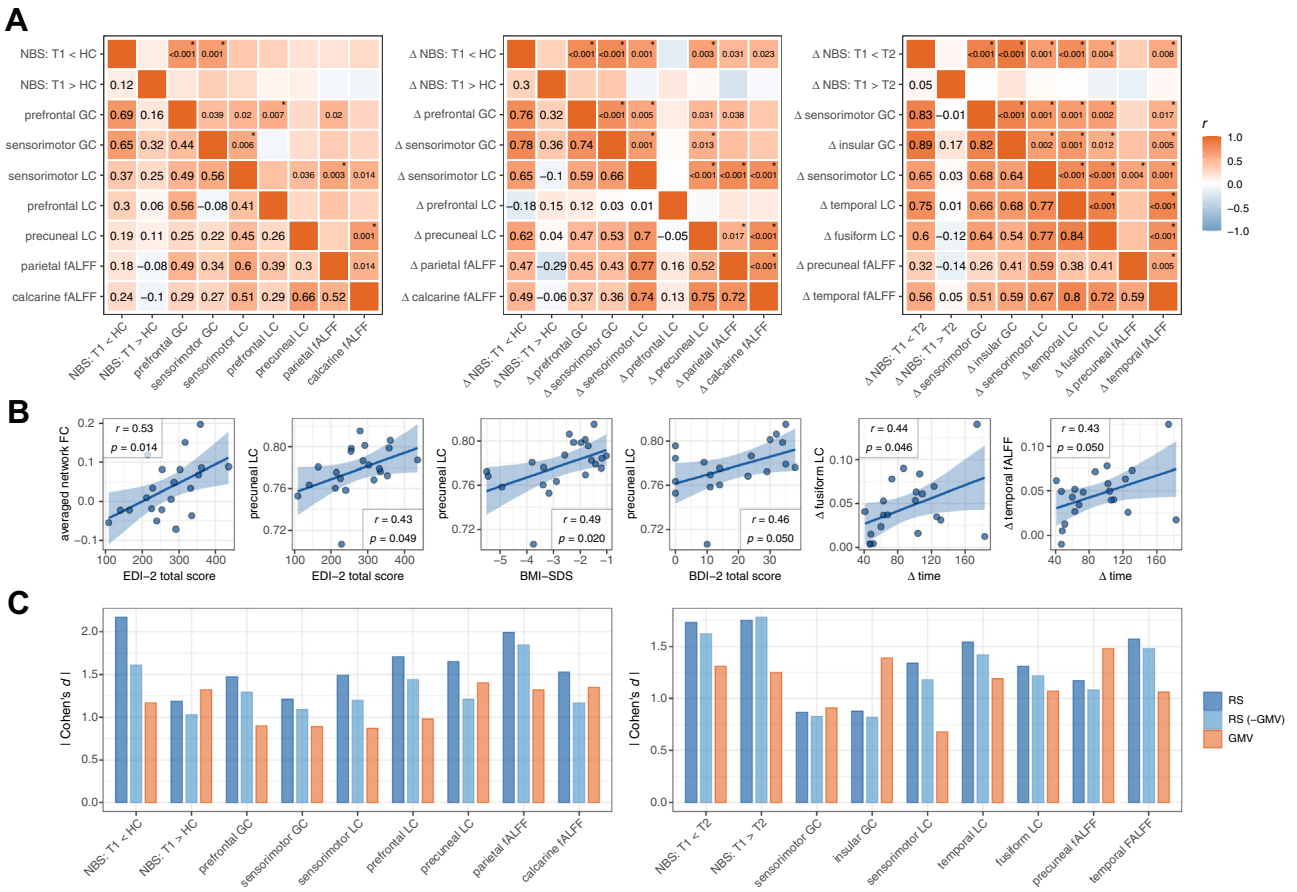


**Figure 3.** Correlations among resting-state measures and with clinical outcome; effect sizes of resting-state group comparisons with and without controlling for voxelwise gray matter volume. **(A)** Left: heatmap representing correlations of resting-state functional magnetic resonance imaging (rsfMRI) results from T1acu vs. HCacu comparison across resting-state measures in the T1acu group. Middle: correlations between T1-T2 changes (Δ) in rsfMRI results from T1acu vs. HCacu comparisons. Right: correlations between T1-T2 changes in rsfMRI results from T1acu vs. T2acu comparisons. Colors of single squares represent the Pearson correlation coefficient *r*. The left lower triangle shows Pearson's *r* values; the right upper triangle shows associated *p* values (if $p > .05$). *Correlations that remained significant after correcting for the false discovery rate (Benjamini-Hochberg procedure). **(B)** 1–4: associations between results from T1acu vs. HCacu rsfMRI comparisons and clinical variables in the acute anorexia nervosa group. 5 and 6: associations between changes in resting-state measures and changes in clinical variables from T1 to T2. Because no correlation survived Bonferroni correction, correlations have to be considered exploratory. Pearson's *r* and uncorrected *p* values are shown. Scatter points represent patients with acute anorexia nervosa at T1 or differences between T1 and T2 (Δ). Blue lines display the fitted linear regression function, blue areas the corresponding 95% confidence interval. **(C)** Effect sizes (Cohen's *d*, Hedge's *g* corrected) from post hoc comparisons of resting-state measures (RS), resting-state measures after voxelwise regression of gray matter volume (RS-GMV) and gray matter volume (GMV). Left: T1acu vs. HCacu; right: T1acu vs. T2acu comparisons. acu, acute; BMI-SDS, body mass index-standard deviation score; EDI-2, Eating Disorder Inventory-2; fALFF, fractional amplitude of low-frequency fluctuations; FC, functional connectivity; GC, global correlation; HC, HCacu (healthy control); LC, local correlation; NBS, network-based statistics; rec, recovered; T, time; T1, T1acu; T2, T2acu.

AN in bilateral prefrontal, sensorimotor, left parietal, left temporal, bilateral precuneal, and insular regions (7–10,20,21,43–47). In contrast to some previous studies, we did not find increases of intraregional (7) or interregional FC and activity (16,17,48–50). This discrepancy may be due to differences in sample size, methodology, and in most cases, shorter illness duration and younger age of our sample (Table S19).

We found a complete normalization of all rsfMRI alterations in long-term recovered patients with a similar trend observed immediately after refeeding therapy. These findings are in line with results of Seidel *et al.* (23) and Cha *et al.* (16) and are further supported by similar conclusions from longitudinal task-based fMRI studies (51,52). This lack of differences between long-term recovered AN and HC in our study further supports the notion that the identified rsfMRI alterations may constitute temporal, presumably starvation-related, state effects of the disorder (23). Differences to previous research indicating persistent alterations in varying brain networks in short- (17) and long-term recovered (18–21) AN may be due to the longer average recovery time (5.3 ± 3 years) and the considerably shorter illness durations in our cohorts (Tables S20 and S21). This further underlines the importance of early identification and treatment of AN during adolescence (2).

Whereas underweight-related GMV decreases in AN were consistently shown (12,13), the dissociation between functional (resting-state) and structural alterations has not been systematically addressed. Our results are supported by preliminary data suggesting decreased function-structure

relationship (7) and GMV independency of resting-state alterations in AN (20). The finding of a global reduction in FC, the normalization of rsfMRI alterations with recovery, and the absence of robust clinical correlations support the notion of rsfMRI alterations being starvation-related phenomena. The missing relationship between resting-state recovery and increasing BMI as well as GMV changes during inpatient treatment may possibly be explained by a mechanism of recovery proceeding faster than weight restoration, such as, for example, short-term changes in energy supply (14,15). The near-absence of resting-state alterations combined with persisting reduced body weight and elevated ED psychopathology at inpatient discharge supports this hypothesis. However, considering the moderate sample size in our study, AN psychopathology may still have an independent influence on recovery of resting-state brain functioning.

Alterations of bilateral prefrontal and left parietal rsfMRI measures display the largest effect sizes in acute AN in our study. Both regions play a central role in altered cognitive control associated with AN pathophysiology as indicated by brain imaging and theoretical and behavioral research (5,6,53,54). Alterations in parietal regions in AN have repeatedly been linked to distorted body image (55). Simultaneously reduced local and global connectivity in prefrontal brain regions point to a common biological background (56,57). In line with that, we detect significant associations between topologically close alterations in different measures and between measures capturing local and global rsfMRI characteristics. In contrast, correlational analyses between changes from T1 to T2 show a much denser pattern of significant correlations across all measures. These findings indicate a global trend of recovery with no notable emphasis on certain resting-state alterations or specific metrics.

As stated above, we did not find correlations between rsfMRI and clinical measures surviving correction for multiple comparisons. Considering the small sample size and the adopted exploratory approach, this was not surprising. Nonetheless, we found some preliminary evidence for associations between rsfMRI and clinical measures, including an unexpected positive correlation between ED severity scales and FC in acute AN that would require replication in larger samples.

### Limitations

A major limitation of this study is the relatively small sample size of the cohort evaluated here, preventing detection of potentially weaker rsfMRI alterations and limiting the generalizability of our findings (58). Furthermore, the AN- and starvation-related differences of pubertal status between patients with acute AN and control subjects and the broad age range of the acute patient group could influence rsfMRI group differences (59,60). Despite these limitations, considering the lack of previous longitudinal rsfMRI studies in AN, our results provide a basis for future hypothesis-driven and replication studies to build on.

### Conclusions

We provided novel insight into the extent and recovery of resting-state brain functioning during the clinical course of AN. Resting-state alterations in AN were independent of GMV and were compatible with starvation-related phenomena, indicating their potential as state markers of the disorder. Consistent with clinical findings, brain regions previously associated with cognitive control and body image disturbance showed the most pronounced alterations in acute AN. Absence of these alterations in our fully recovered group with relatively short illness duration underlines the importance of early identification and treatment in AN.

## ACKNOWLEDGMENTS AND DISCLOSURES

The study was supported by the Swiss Anorexia Nervosa Foundation (cohort 2; Grant No. 53-15 [to KK]).

LDL performed all analyses and wrote the manuscript with support of JD and GvP. LDL, KK, SBE, JS, and JD designed the overall study. JO, KB, LS, and LDL conducted the clinical studies and gathered the data under the supervision of JS and KK. All authors reviewed and commented on the manuscript.

A previous version of this article was published as a preprint on medRxiv: https://doi.org/10.1101/2020.06.21.20135566.

Statistical group-level maps derived from the reported analyses were uploaded to NeuroVault (https://neurovault.org/collections/EIFQNRMC/).

JD is a former employee and received consultancy fees on another topic from F. Hoffmann-La Roche AG. All other authors report no biomedical financial interests or potential conflicts of interest.

## ARTICLE INFORMATION

From the Child Neuropsychology Section (LDL, JO, KK), Department of Child and Adolescent Psychiatry, Psychosomatics and Psychotherapy (GvP, KB, LS, JS), University Hospital RWTH Aachen, Aachen; Institute of Neuroscience and Medicine, Brain & Behaviour (INM-7) (LDL, GvP, SBE, JD), Research Centre Jülich; JARA-Brain Institute II (KK), Molecular Neuroscience and Neuroimaging, Research Centre Jülich, Jülich; and Institute of Systems Neuroscience (LDL, GvP, SBE, JD), Medical Faculty, Heinrich Heine University Düsseldorf, Düsseldorf, Germany.

JS and JD contributed equally to this work.

Address correspondence to Leon D. Lotter., at leon.lotter@rwth-aachen.de or leondlotter@gmail.com.

Received Feb 11, 2021; revised Feb 16, 2021; accepted Mar 4, 2021.

Supplementary material cited in this article is available online at https://doi.org/10.1016/j.bpsc.2021.03.006.

3D neuroimaging content is available for this article online at https://doi.org/10.1016/j.bpsc.2021.03.006.

## REFERENCES

1. American Psychiatric Association (2013): Diagnostic and Statistical Manual of Mental Disorders (DSM–5). Arlington: American Psychiatric Publishing.
2. Zipfel S, Giel KE, Bulik CM, Hay P, Schmidt U (2015): Anorexia nervosa: Aetiology, assessment, and treatment. Lancet Psychiatry 2:1099–1111.
3. Damoiseaux JS, Rombouts SARB, Barkhof F, Scheltens P, Stam CJ, Smith SM, Beckmann CF (2006): Consistent resting-state networks across healthy subjects. Proc Natl Acad Sci U S A 103:13848–13853.
4. Fox MD, Greicius M (2010): Clinical applications of resting state functional connectivity. Front Syst Neurosci 4:19.
5. Gaudio S, Olivo G, Beomonte Zobel B, Schiöth HB (2018): Altered cerebellar-insular-parietal-cingular subnetwork in adolescents in the earliest stages of anorexia nervosa: A network-based statistic analysis. Transl Psychiatry 8:127.
6. Gaudio S, Wiemerslage L, Brooks SJ, Schiöth HB (2016): A systematic review of resting-state functional-MRI studies in anorexia nervosa: Evidence for functional connectivity impairment in cognitive control and visuospatial and body-signal integration. Neurosci Biobehav Rev 71:578–589.

7. Steward T, Menchon JM, Jiménez-Murcia S, Soriano-Mas C, Fernandez-Aranda F (2018): Neural network alterations Across eating disorders: A narrative review of fMRI studies. Curr Neuropharmacol 16:1150–1163.
8. Seidel M, Borchardt V, Geisler D, King JA, Boehm I, Pauligk S, *et al.* (2019): Abnormal spontaneous regional brain activity in young patients with anorexia nervosa. J Am Acad Child Adolesc Psychiatry 58:1104–1114.
9. Kullmann S, Giel KE, Teufel M, Thiel A, Zipfel S, Preissl H (2014): Aberrant network integrity of the inferior frontal cortex in women with anorexia nervosa. Neuroimage Clin 4:615–622.
10. Ehrlich S, Lord AR, Geisler D, Borchardt V, Boehm I, Seidel M, *et al.* (2015): Reduced functional connectivity in the thalamo-insular subnetwork in patients with acute anorexia nervosa. Hum Brain Mapp 36:1772–1781.
11. Hebebrand J, Muller TD, Holtkamp K, Herpertz-Dahlmann B (2007): The role of leptin in anorexia nervosa: Clinical implications. Mol Psychiatry 12:23–35.
12. Seitz J, Bühren K, von Polier GG, Heussen N, Herpertz-Dahlmann B, Konrad K (2014): Morphological changes in the brain of acutely ill and weight-recovered patients with anorexia nervosa. A meta-analysis and qualitative review. Z Kinder Jugendpsychiatr Psychother 42:7–17; quiz 17–18.
13. Seitz J, Herpertz-Dahlmann B, Konrad K (2016): Brain morphological changes in adolescent and adult patients with anorexia nervosa. J Neural Transm (Vienna) 123:949–959.
14. Al-Zubaidi A, Heldmann M, Mertins A, Jauch-Chara K, Münte TF (2018): Influences of hunger, satiety and oral glucose on functional brain connectivity: A multimethod resting-state fMRI study. Neuroscience 382:80–92.
15. Al-Zubaidi A, Iglesias S, Stephan KE, Buades-Rotger M, Heldmann M, Nolde JM, *et al.* (2020): Effects of hunger, satiety and oral glucose on effective connectivity between hypothalamus and insular cortex. Neuroimage 217:116931.
16. Cha J, Ide JS, Bowman FD, Simpson HB, Posner J, Steinglass JE (2016): Abnormal reward circuitry in anorexia nervosa: A longitudinal, multimodal MRI study. Hum Brain Mapp 37:3835–3846.
17. Uniacke B, Wang Y, Biezonski D, Sussman T, Lee S, Posner J, Steinglass J (2019): Resting-state connectivity within and across neural circuits in anorexia nervosa. Brain Behav 9:e01205.
18. Boehm I, Geisler D, Tam F, King JA, Ritschel F, Seidel M, *et al.* (2016): Partially restored resting-state functional connectivity in women recovered from anorexia nervosa. J Psychiatry Neurosci 41:377–385.
19. Cowdrey FA, Filippini N, Park RJ, Smith SM, McCabe C (2014): Increased resting state functional connectivity in the default mode network in recovered anorexia nervosa. Hum Brain Mapp 35:483–491.
20. Favaro A, Santonastaso P, Manara R, Bosello R, Bommarito G, Tenconi E, Di Salle F (2012): Disruption of visuospatial and somatosensory functional connectivity in anorexia nervosa. Biol Psychiatry 72:864–870.
21. Scaife JC, Godier LR, Filippini N, Harmer CJ, Park RJ (2017): Reduced resting-state functional connectivity in current and recovered restrictive anorexia nervosa. Front Psychiatry 8:30.
22. Dukart J, Sambataro F, Bertolino A (2017): Distinct role of striatal functional connectivity and dopaminergic loss in Parkinson's symptoms. Front Aging Neurosci 9:151.
23. Seidel M, Geisler D, Borchardt V, King JA, Bernardoni F, Jaite C, *et al.* (2020): Evaluation of spontaneous regional brain activity in weight-recovered anorexia nervosa. Transl Psychiatry 10:395.
24. Zalesky A, Fornito A, Bullmore ET (2010): Network-based statistic: Identifying differences in brain networks. Neuroimage 53:1197–1207.
25. Whitfield-Gabrieli S, Nieto-Castanon A (2012): Conn: A functional connectivity toolbox for correlated and anticorrelated brain networks. Brain Connect 2:125–141.
26. Deshpande G, LaConte S, Peltier S, Hu X (2009): Integrated local correlation: A new measure of local coherence in fMRI data. Hum Brain Mapp 30:13–23.
27. Zou QH, Zhu CZ, Yang Y, Zuo XN, Long XY, Cao QJ, *et al.* (2008): An improved approach to detection of amplitude of low-frequency fluctuation (ALFF) for resting-state fMRI: Fractional ALFF. J Neurosci Methods 172:137–141.
28. Hilbert A, Tuschen-Caffier B, Ohms M (2004): Eating Disorder Examination: Deutschsprachige Version des strukturierten Essstörungsinterviews. Diagnostica 50:98–106.
29. Paul T, Thiel A (2005): EDI-2. Eating Disorder Inventory-2. Göttingen, Germany: Hogreve.
30. Hemmelmann C, Brose S, Vens M, Hebebrand J, Ziegler A (2010): Perzentilen des Body-Mass-Index auch für 18- bis 80-Jährige? Daten der Nationalen Verzehrsstudie II [Percentiles of body mass index of 18-80-year-old German adults based on data from the Second National Nutrition Survey. Dtsch Med Wochenschr 135:848–852.
31. Neuhauser H, Schienkiewitz A, Schaffrath-Rosario A, Dortschy R, Kurth BM (2013): Referenzperzentile Für Anthropometrische Maßzahlen Und Blutdruck Aus Der Studie Zur Gesundheit von Kindern Und Jugendlichen in Deutschland (KiGGS), Version 2. Berlin, Germany: Robert Koch Institut.
32. Hautzinger M, Keller F, Kühner C (2009): Beck-Depressions-Inventar. Revision. 2. Frankfurt: Auflage. Pearson Assessment.
33. Delmo C, Weiffenbach O, Gabriel M, Poustka F (2000): Kiddie-SADS-present and lifetime version (K-SADS-PL), German adaptation, 2001, Klinik für Psychiatrie und Psychotherapie des Kindes-und Jugendalters der Universität Frankfurt. Germany: Frankfurt am Main.
34. Ackenheil M, Stotz G, Dietz-Bauer R (1999): Mini International Neuropsychiatric Interview. German Version 5.0.0, DSM-IV. München: Psychiatrische Universitätsklinik München.
35. Lehrl S (2005): Mehrfachwahl-Wortschatz-Intelligenztest MWT-B, Edition 5. Balingen: Spitta Verlag.
36. The FIL Methods Group: Statistical Parametric Mapping, Version 12. Available at: https://www.fil.ion.ucl.ac.uk/spm/.
37. Friston KJ, Williams S, Howard R, Frackowiak RSJ, Turner R (1996): Movement-related effects in fMRI time-series. Magn Reson Med 35:346–355.
38. R Foundation: The R project for statistical computing Available at: https://www.R-project.org/.
39. Jamovi Available at: https://www.jamovi.org.
40. Eklund A, Nichols TE, Knutsson H (2016): Cluster failure: Why fMRI inferences for spatial extent have inflated false-positive rates. Proc Natl Acad Sci U S A 113:7900–7905.
41. Schaefer A, Kong R, Gordon EM, Laumann TO, Zuo XN, Holmes AJ, *et al.* (2018): Local-global parcellation of the human cerebral cortex from intrinsic functional connectivity MRI. Cereb Cortex 28:3095–3114.
42. Rolls ET, Huang CC, Lin CP, Feng J, Joliot M (2020): Automated anatomical labelling atlas 3. Neuroimage 206:116189.
43. Gaudio S, Piervincenzi C, Beomonte Zobel B, Romana Montecchi F, Riva G, Carducci F, Quattrocchi CC (2015): Altered resting state functional connectivity of anterior cingulate cortex in drug naïve adolescents at the earliest stages of anorexia nervosa. Sci Rep 5:10818.
44. Geisler D, Borchardt V, Lord AR, Boehm I, Ritschel F, Zwipp J, *et al.* (2016): Abnormal functional global and local brain connectivity in female patients with anorexia nervosa. J Psychiatry Neurosci 41:6–15.
45. Haynos AF, Hall LMJ, Lavender JM, Peterson CB, Crow SJ, Klimes-Dougan B, *et al.* (2019): Resting state functional connectivity of networks associated with reward and habit in anorexia nervosa. Hum Brain Mapp 40:652–662.
46. Phillipou A, Abel LA, Castle DJ, Hughes ME, Nibbs RG, Gurvich C, Rossell SL (2016): Resting state functional connectivity in anorexia nervosa. Psychiatry Res Neuroimaging 251:45–52.
47. de la Cruz F, Schumann A, Suttkus S, Helbing N, Zopf R, Bär KJ (2021): Cortical thinning and associated connectivity changes in patients with anorexia nervosa. Transl Psychiatry 11:95.
48. Biezonski D, Cha J, Steinglass J, Posner J (2016): Evidence for thalamocortical circuit abnormalities and associated cognitive dysfunctions in underweight individuals with anorexia nervosa. Neuropsychopharmacology 41:1560–1568.
49. Boehm I, Geisler D, King JA, Ritschel F, Seidel M, Deza Araujo Y, *et al.* (2014): Increased resting state functional connectivity in the fronto-parietal and default mode network in anorexia nervosa. Front Behav Neurosci 8:346.
50. Lee S, Ran Kim K, Ku J, Lee JH, Namkoong K, Jung YC (2014): Resting-state synchrony between anterior cingulate cortex and

precuneus relates to body shape concern in anorexia nervosa and bulimia nervosa. Psychiatry Res 221:43–48.
51. Decker JH, Figner B, Steinglass JE (2015): On weight and waiting: Delay discounting in anorexia nervosa pretreatment and posttreatment. Biol Psychiatry 78:606–614.
52. Doose A, King JA, Bernardoni F, Geisler D, Hellerhoff I, Weinert T, *et al.* (2020): Strengthened default mode network activation during delay discounting in adolescents with anorexia nervosa after partial weight restoration: A longitudinal fMRI study. J Clin Med 9:900.
53. Kaye WH, Wierenga CE, Bailer UF, Simmons AN, Bischoff-Grethe A (2013): Nothing tastes as good as skinny feels: The neurobiology of anorexia nervosa. Trends Neurosci 36:110–120.
54. Fuglset TS (2019): Set-shifting, central coherence and decision-making in individuals recovered from anorexia nervosa: A systematic review. J Eat Disord 7:22.
55. Gaudio S, Quattrocchi CC (2012): Neural basis of a multidimensional model of body image distortion in anorexia nervosa. Neurosci Biobehav Rev 36:1839–1847.
56. Deco G, Ponce-Alvarez A, Hagmann P, Romani GL, Mantini D, Corbetta M (2014): How local excitation-inhibition ratio impacts the whole brain dynamics. J Neurosci 34:7886–7898.
57. Vuksanović V, Hövel P (2014): Functional connectivity of distant cortical regions: Role of remote synchronization and symmetry in interactions. Neuroimage 97:1–8.
58. Poldrack RA, Baker CI, Durnez J, Gorgolewski KJ, Matthews PM, Munafò MR, *et al.* (2017): Scanning the horizon: Towards transparent and reproducible neuroimaging research. Nat Rev Neurosci 18:115–126.
59. Petersen N, Kilpatrick LA, Goharzad A, Cahill L (2014): Oral contraceptive pill use and menstrual cycle phase are associated with altered resting state functional connectivity. Neuroimage 90:24–32.
60. Faghiri A, Stephen JM, Wang YP, Wilson TW, Calhoun VD (2019): Brain development includes linear and multiple nonlinear trajectories: A cross-sectional resting-state functional magnetic resonance imaging study. Brain Connect 9:777–788.